Turkish Journal of Electrical Engineering & Computer Sciences

http://journals.tubitak.gov.tr/elektrik/

Research Article

Turk J Elec Eng & Comp Sci
(2014) 22: 1501 – 1516

doi:10.3906/elk-1212-143

# A new PSFB converter-based inverter arc welding machine with high power density and high efficiency

**İsmail AKSOY***
Department of Electrical Engineering, Yıldız Technical University, Davutpaşa Campus, Esenler, İstanbul, Turkey

**Received:** 25.12.2012 • **Accepted:** 28.01.2013 • **Published Online:** 07.11.2014 • **Printed:** 28.11.2014

**Abstract:** In this study, a high-performance single-phase inverter arc welding machine is presented. Power control of the developed welding machine is realized with a high-frequency, phase-shifted full bridge (PSFB) pulse-width modulation (PWM) converter. The PSFB PWM converter operates with soft switching at no load and full load. There is no need to use a passive snubber in the converter. Welding machine control is implemented with a digital signal processor (DSP) and phase-shift PWM IC. By means of the DSP, advanced arc welding functions and protection features such as short-circuit, over-current, and temperature protection are achieved. The current and voltage waveforms given are from an IGBT-based PSFB PWM arc welding machine operating at 75 kHz switching frequency and 160 A output current. The experimental results show that the proposed system has promising feasibility in industrial applications.

**Key words:** Arc welding machine, PSFB PWM converter, DC-DC converter, soft switching, zero-voltage transition, zero-voltage switching, IGBT

## 1. Introduction

An arc welding machine provides the required current and voltages at different stages of the arc process. Initially, high voltage is produced at no load, which is also called open-circuit voltage. When the electrode is touched to the piece a short circuit occurs and the current increases suddenly. After the output current reaches the reference current level, the arc welding machine regulates the output voltage to maintain a constant current, which is required for metal transfer. The voltage produced in the steady state is proportional to the current, which depends on the arc length and electrode diameter. During the transient state of the arc process, the load varies between open circuit and short circuit [1].

In welding machines, a transformer is used for voltage transformation and isolation, and inductance is used at the output stage to filter output current. Currently, high-frequency inverter welding machines are preferred to conventional welding machines due to their high efficiency and high performance. The converter should operate at high frequency in order to realize high-performance control and decrease the size of magnetic elements. By means of high frequency operation, the converter volume and output current ripple decrease. Welding quality is improved due to the fast response of the system to sudden changes in load during the welding process. The converter can be operated at high frequency by means of soft switching techniques [2].

MOSFETs or IGBTs can be utilized in inverter welding machines. The MOSFET, which is the preferred switching power device at high frequencies, suffers from high switching turn-on loss due to its high-value parasitic

*Correspondence: iaksoy@yildiz.edu.tr

capacitor. In the isolated pulse-width modulation (PWM) DC-DC converters, transformer leakage inductance leads to switching losses when the converter operates with hard switching and decreases efficiency of the circuit due to the requirement of passive snubber elements. The phase-shift PWM (PSPWM) method is proposed to solve these problems. In this method, a quasiresonance is formed between the parasitic capacitance of power switches and transformer leakage inductance so that the leakages are utilized beneficially, and soft switching is obtained. In this topology the energy stored in inductance is used for the discharging of the parasitic capacitors of the MOSFET. The MOSFET is turned on with zero-voltage transition (ZVT) and turned off with zero-voltage switching (ZVS). In the conventional PSPWM method, the soft-switching range is limited due to the insufficient energy of the leakage inductance at low currents. The parasitic capacitor of the MOSFET is not discharged at low load currents. In addition, the output diodes are exposed to excessive voltage stress in the phase-shifted full bridge (PSFB) PWM converter. In order to solve these problems, many approaches have been proposed in the literature [3–40].

In industrial applications at high voltage and high power levels, the IGBT is preferred over MOSFET. Due to the high resistance of the MOSFET at high voltage levels, the conduction losses increase and the converter efficiency decreases. For these reasons, as well as for economic considerations, IGBTs are preferred to MOSFETs in industrial applications. However, the tail current problem associated with IGBTs limits their use in high-frequency and high-power applications. In the PSPWM, converter turn-off losses of the MOSFET are reduced by its parasitic capacitor. When the IGBT is used instead of the MOSFET, additional snubber capacitors are required to reduce the switching losses of the IGBT in the turn-off process [6–8].

It is assumed that the IGBT is turned off under ZVS with a high-value parallel capacitor. In a no-load or light-load situation, the ZVT condition is not provided. In these cases, the parallel capacitors discharge through the IGBT when it is turned on. This is the reason for the increase in switching losses and failure risk in IGBTs [9–23]. The use of a high-value capacitor in parallel with the IGBT is restricted because of the capacitor discharge through the IGBT. Therefore, the selection of the parallel capacitor value is very important [33–34].

In high-power applications such as welding machines, isolated DC-DC converters are preferred. In these converters, a high-frequency AC voltage is produced with an inverter, the AC voltage is rectified by diodes, and the output current is filtered by inductance. The power topology used in the inverter welding machines is selected depending on price, performance, control complexity, and implementation difficulty. Half-bridge (HB), full-bridge (FB), and 2-switch forward topologies are widely used in inverter welding machines. The 2-switch forward converter magnetizes the transformer in 1 direction; thus, the transformer B-H curve is not fully utilized. The HB DC-DC converter is known as the simplest isolated converter, but use of this converter is limited at high power levels. The FB DC-DC converter is more suitable for high-power welding machines [41].

In this study, a high-performance digital signal processor (DSP)-controlled new single-phase arc welding machine is presented. The power conversion in the developed welding machine is realized with a PSFB high-frequency PWM converter. Theoretical analysis and the operating modes of the converter are given. Phase-shift PWM IC and DSP are used to control the welding machine. Arc welding functions are analyzed with simulation and implemented with the DSP in the welding machine. The operation principles, theoretical analysis, and simulation results are completely verified by a prototype welding machine with 5 kW output power, 160 A output current, and 75 kHz switching frequency.

## 2. Operation principles of the PSFB PWM converter

The IGBT-based PSFB PWM converter in [42] is used in the proposed welding machine. In this converter, high-value capacitors can be connected in parallel to the power switches in the leading leg to provide soft switching. However, the use of high-value capacitors in the lagging leg causes problems. In no-load or light-load situations, the ZVT condition is not provided. In this case, the parallel capacitors discharge through the IGBT when it is turned on. Most of the problems occur at the lagging leg [3–23]. If the parallel capacitor values of the lagging leg IGBTs are not sufficient, switching losses reach unacceptable levels at high currents. PSFB PWM DC-DC converter performance decreases due to the increase in switching losses. This results in performance degradation and the reduction of machine duty at high currents. To solve this problem, a new method that enables the use of high-value capacitors with the lagging leg of the PSFB PWM converter without any problems is proposed. The proposed converter decreases the turn-off switching losses at high currents and improves the performance of the welding machine. The proposed arc welding machine circuit is shown in Figure 1. It consists of a conventional PSFB PWM converter and an auxiliary circuit. Auxiliary switches operate under soft switching, and their conduction losses are very low. The turn-off performance of the lagging leg IGBTs is improved by the auxiliary circuit. The power converter operates as the conventional PSFB PWM converter at low output currents. The operation of the auxiliary circuit starts when the primary current ($I_p$) is larger than a predetermined current level ($I_a$). This level depends on the nominal current of the converter and characteristics of the power switches. When the current falls below $I_a$, the converter returns to conventional operation.

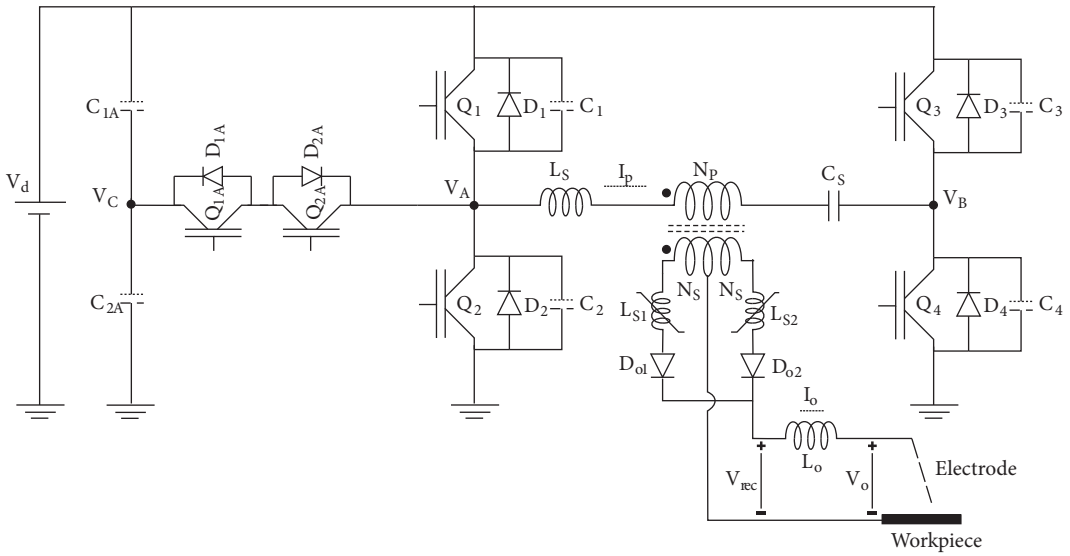


**Figure 1.** The PSFB PWM converter used in an arc welding machine.

In theoretical analysis, input voltage $V_d$ and output current $I_o$ are constant, and the parallel snubber capacitors are ideal. The proposed arc welding machine circuit has 6 operating intervals within each half-cycle. The equivalent circuits for each operating stage are shown in Figures 2a–2f.

Interval 1 ($t_o < t < t_1$, Figure 2a): $Q_1$ and $Q_4$ switches are conducting, and power is transferred to the output at the beginning of this interval. The diode $D_{o1}$ is in the on state, and output current flows through it. The value of $V_C$ is equal to the input voltage. The control signal of $Q_4$ is removed and $Q_4$ starts to turn off at $t = t_0$. There is a delay, defined as $t_{doff}$, at the beginning of the turn-off process. In this interval the currents of $Q_1$ and $Q_4$ are equal to $I_P$. $Q_4$ is still in the on state, and current flows through the IGBT.

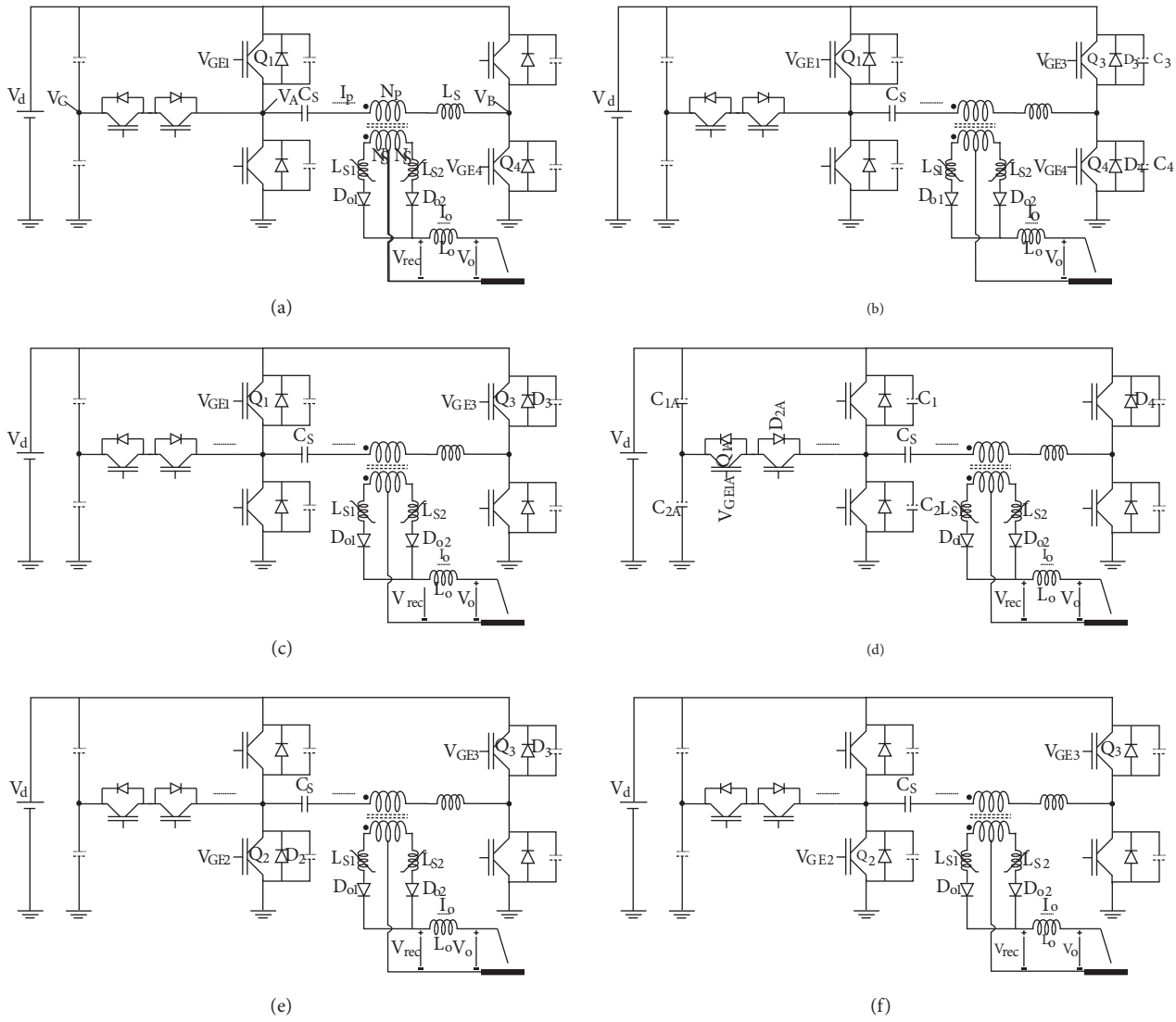


**Figure 2.** Equivalent circuits of the welding machine.

Interval 2 ($t_1 < t < t_2$, Figure 2b): After $t = t_1$, first the current of $Q_4$ starts to decrease, and it falls to the tail current value at the end of $t_f$. There is a little increase in the voltage of $Q_4$ due to the parallel capacitors in this interval. The turn-off loss of $Q_4$ is very low. The equivalent capacitor value $C_p$ is equal to the sum of $C_3$ and $C_4$.

Interval 3 ($t_2 < t < t_4$, Figure 2c): At $t = t_2$, the $D_3$ diode turns on, and this interval starts. The control signal of $Q_3$ can be applied after turning on $D_3$. The application of the control signal should occur before $I_P$ becomes zero. $Q_1$ and $D_3$ are conducting in this interval. At $t = t_3$, the control signal of $Q_1$ is removed.

Interval 4 ($t_4 < t < t_5$, Figure 2d): Lagging leg transition begins at $t = t_4$. The value of the primary current is $I_{P0}$. In this stage, according to $I_p$ level, 2 different operation modes exist. In operation mode 1, the auxiliary circuit is not activated if the primary current is smaller than $I_a$. This mode of the proposed converter would have a conventional operation. In operation mode 2, the auxiliary circuit is operated if the primary current is larger than $I_a$. Soft switching is obtained at high current levels due to additional high-valued

capacitors. By the discharge of the capacitor ($C_2$ // $C_{2A}$) through the resonance between $L_S$ and $C_P$, this interval is completed, and the primary current falls to the $I_{P1}$ level.

Interval 5 ($t_5 < t < t_7$, Figure 2e): At $t = t_5$, the $D_2$ diode is turned on, the voltage across $L_S$ is negative, and the current falls to zero linearly. The control signal of $Q_2$ can be applied after diode $D_2$ turns on. At $t = t_6$, the auxiliary switch control signal is removed. When the primary current falls to zero, this interval is finished.

Interval 6 ($t_7 < t < t_8$, Figure 2f): The primary current decreases from 0 to $-I_o/a$ in this interval. At $t = t_8$, the current of diode $D_{o1}$ falls to zero, and output current flows through diode $D_{o2}$. After $t_8$, standard PWM operation takes place, and power is transferred to the output. In the second half-cycle, a symmetrical operation occurs, and after this a new switching period starts.

## 3. Simulation results of the developed arc welding machine

The arc welding process is composed of many states, such as open circuit, short circuit, generation of arc voltage, and change of arc voltage during welding. Before starting to weld, the user adjusts the reference current value according to the diameter and type of the electrode. The welding process starts when the electrode is touched to the piece, a short circuit occurs, and the current increases suddenly. The high current causes the electrode to melt and generates an arc.

Initially, a current that is higher than the reference current is forced in a short period to prevent the sticking of the electrode and pieces and to accelerate the generation of arc. This is called a hot-start process. The current value and duration are determined according to the diameter and type of the electrode in the hot-start process. After the hot-start process, the current is reduced to its reference value. The arc voltage is proportional to arc length and varies depending on the welder's hand movements during welding. If the electrode distance is too long, the arc extinguishes. If the electrode is touched to the piece, a short circuit occurs. The user must keep the distance between the electrode and the piece within a certain range for welding quality. By means of current control, welding current is stabilized against the fluctuations in the arc voltage. The current control also provides compensation against DC bus voltage and grid voltage fluctuations. If a short circuit occurs during welding, the current reference is made maximum for a short period to remove the short circuit. If the short circuit is removed at the end of this period, the current reference is set to its normal value. Otherwise, the current reference is set to zero. In this condition, the user can easily separate the sticking electrode from the piece. The welding process restarts with touching the electrode. In conventional transformer welding machines, separating the stuck electrode from the piece is quite difficult. User-friendly features can be implemented with software due to the high-speed current and voltage control characteristics of the inverter welding machines.

In order to investigate the characteristics of the arc welding, a simulation is performed in MATLAB. The basic structure of the system is shown in Figure 3. The system consists of a PSPWM DC-DC converter, arc welding model, and arc welding and PI current control algorithms. By changing the arc voltage during the simulation, the operation of the system is investigated. In the PSPWM converter, the input voltage is 300 V and the switching frequency is 75 kHz. High-frequency transformer output voltage is rectified by diodes. The pulse frequency of the rectified $V_{rec}$ voltage is 150 kHz. The average value of the output voltage is changed by the duty cycle and output current is controlled. The current ripple is reduced with an inductance connected in series with the output. The current control can be implemented precisely by means of high-frequency operation. The operating frequency of the DC-DC converter is high enough in respect to the arc welding dynamics. At no-load, the welding machine output voltage is at a maximum. The PSPWM converter transformer conversion

ratio is 5:1; as a result, the maximum value of output voltage is 60 V. During welding, current control is provided by adjusting the output voltage at $20 < V_{rec} < 60$ V.

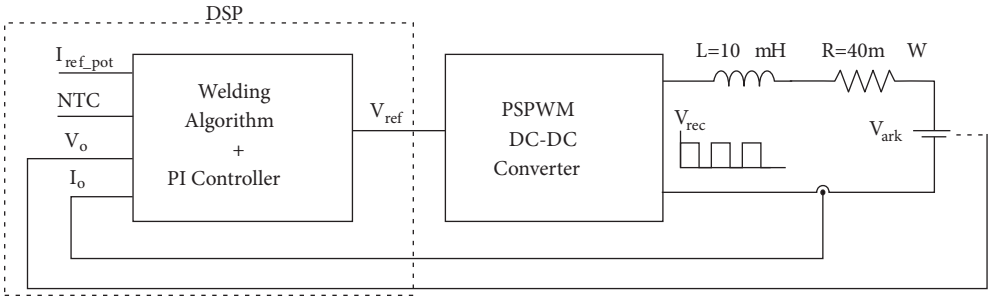


**Figure 3.** Block diagram of the system.

The welding algorithm and PI current control was realized with DSP software. The welding algorithm produces the current reference at the initial state, normal welding, and short-circuit state. The PI controller produces the reference voltage ($V_{ref}$) to follow the current reference. The reference ($V_{ref}$) that is produced by DSP is applied to the UC3879 chip. The PSPWM converter is controlled by the UC3879 chip. The output current and arc voltage waveforms from the MATLAB simulation are shown in Figure 4. The initial operating voltage is 60 V at no-load. The current reference ($I_{ref}$) is set to 100 A. At t = 0.5 ms, with the beginning of welding, arc voltage ($V_{arc}$) becomes 20 V. Hand movements of the welder are represented by changing the arc voltage in the simulation. Initially, a high current (160 A) flows for a short time. After the hot-start process, the current reference ($I_{ref}$) falls to 100 A, and the normal welding process starts. This stage can continue until electrode melting is completed. Afterwards, at t = 2.5 ms, a short circuit is generated. The current reference is set to a maximum value of 300 $\mu$s after the short circuit. The short circuit continues for a long time; thus, the current reference is set at zero. The output voltage rises to 60 V when the electrode is unstuck from the piece. At t = 4 ms, the electrode is touched to the piece, and the welding process restarts with a hot start. After the hot-start duration, the reference current falls to its normal value at t = 4.5 ms. A short circuit occurs between 5.2 ms and 5.5 ms. This short circuit is eliminated by applying maximum current. The current reference is reduced to the normal value and the welding operation continues. The waveforms obtained for different current references by simulation are shown in Figures 5–7. At t = 0.5 ms, welding starts after the hot-start duration, and the current reference is reduced to a normal value. In Figure 5, the output current and arc voltage waveforms are given for $I_{ref}$ = 125 A. The output current is not affected by the fluctuations of arc voltage $V_{arc}$.

The output current and arc voltage waveforms are shown in Figures 6 and 7 for $I_{ref}$ = 100 A and $I_{ref}$ = 50 A, respectively. The dynamic response of the current is quite fast, and output current ripple is extremely low due to the high-frequency operation. The reference voltage is produced by the 9-bit DAC of the DSP. In Figures 5–7, it is seen that the maximum reference voltage corresponds to the number 512.

MATLAB simulations constitute a basis for the software required for welding machine control. During software development, the PROTEUS program is utilized. The simulation of arc welding realized using the PROTEUS program is given in Figure 8. In the simulation model $V_{arc}$ is defined as a variable controlled source. The arc voltage during welding, short circuit, and open circuit are modeled as 20 V, 0 V, and 60 V, respectively. An equivalent buck converter is used instead of a PSPWM converter model to simplify the analysis. Output inductance is 10 $\mu$H, and the output resistance is 40 m$\Omega$. The control signal is produced from the PWM2H1 output of DSP. PWM_filt is the filtered value of the PWM signal. PWM1H1 is used for

test purposes. A high-frequency PWM signal is applied to the RC filter and a DAC circuit is obtained. It is possible to follow the software variables with the test output. The operation of auxiliary circuits in the PSPWM converter is controlled by the Stop_Aux output. PSPWM DC-DC converter control, welding control, closed-loop PI current control, and temperature protection are realized with the developed DSP software. After PROTEUS simulations, the required application software is completed with experiments on the welding machine.

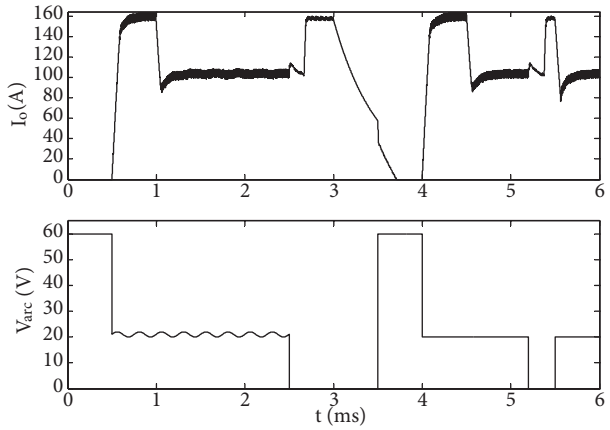


**Figure 4.** The output current and arc voltage waveforms.

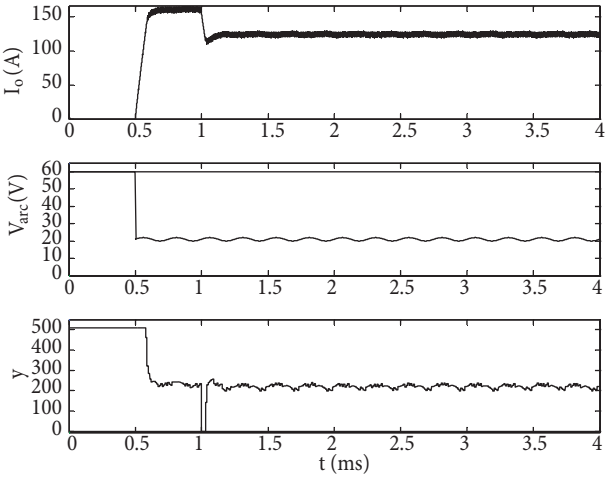


**Figure 5.** The output current, arc voltage, and reference voltage waveforms for $I_{ref}$ = 125 A.

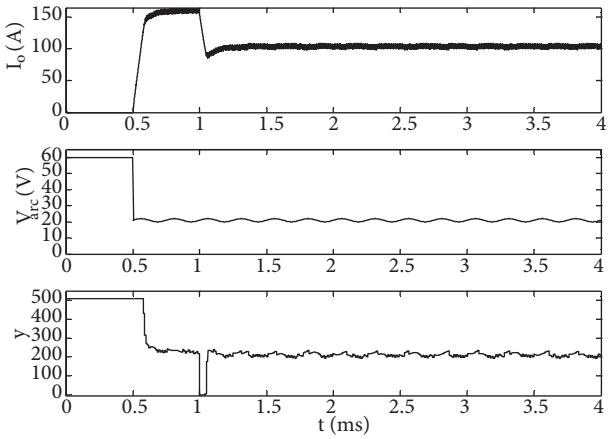


**Figure 6.** The output current, arc voltage, and reference voltage waveforms for $I_{ref}$ = 100 A.

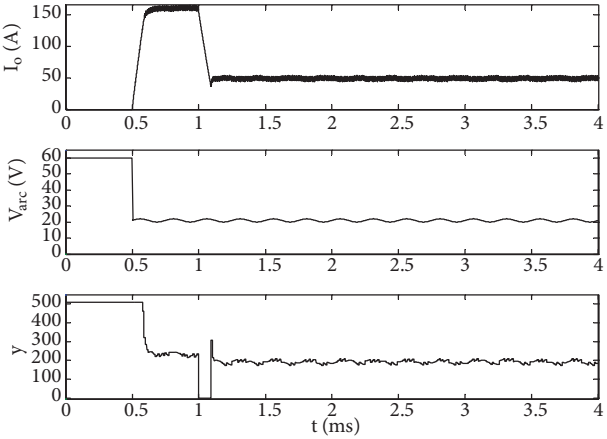


**Figure 7.** The output current, arc voltage, and reference voltage waveforms for $I_{ref}$ = 50 A.

In the PSPWM DC-DC converter, DC link voltage is obtained by rectifying and filtering the single-phase grid voltage. In the simulation model shown in Figure 8, the gain of E1 is selected as 12. PWM changes between 0 and 5 V; thus, the voltage produced at the output of E1 changes between 0 and 60 V. E2 represents $V_{arc}$, and it is controlled by $V_{g\_arc}$. The gain of controlled voltage source E2 is selected as unity.

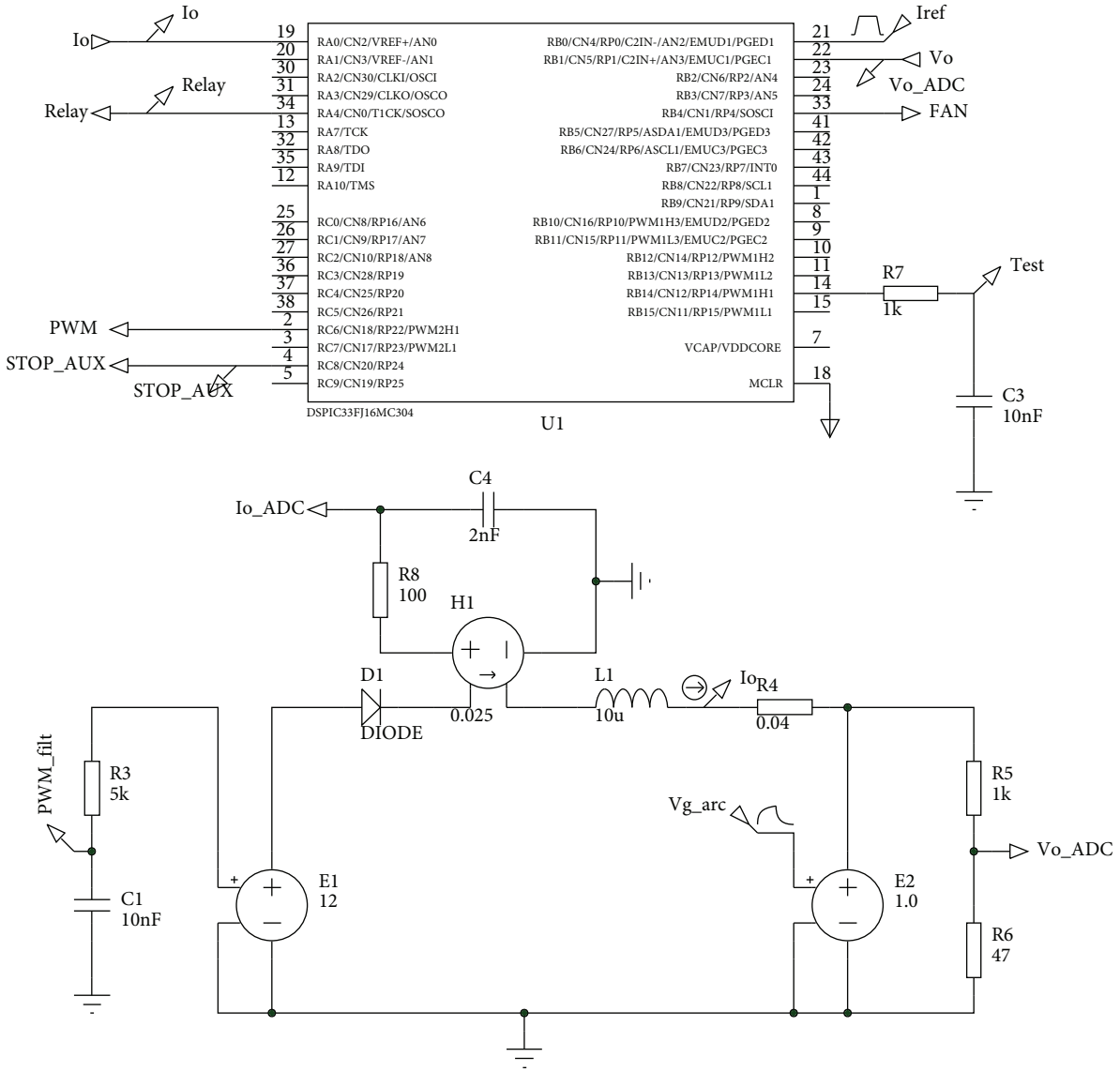


**Figure 8.** Arc welding simulation in PROTEUS.

One control cycle takes 9.4 $\mu$s. The executed processes in the DSP in one control cycle are summarized below sequentially.

Output current, output voltage, reference current, and temperature information from the NTC are read by the ADC. The start/stop operation of the auxiliary circuit is determined depending on the output current level in the PSPWM converter. Additionally, the fan is controlled based on the temperature and, if necessary, the power circuit is shut down. In Figures 9 and 10, the arc welding simulation waveforms obtained in the PROTEUS program are shown. In Figure 10, it is seen that the output current is controlled according to the welding voltage, which is given Figure 9. If the output current exceeds 100 A, an auxiliary circuit is started. If the output current falls below 90 A, the auxiliary circuit is stopped. Thus, the switching losses of the lagging IGBTs are reduced at high current levels, and the soft-switching range is extended. The results obtained from the PROTEUS program are similar to the MATLAB simulation results. The current and welding controls, which are implemented with DSP software, are realized successfully in the simulation environment.

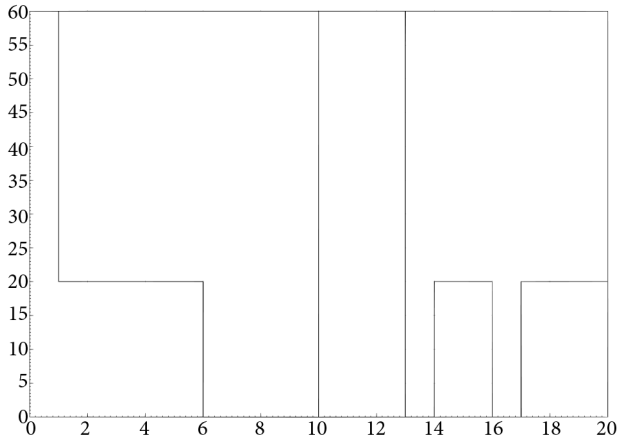


**Figure 9.** $V_{arc}$ voltage in PROTEUS.

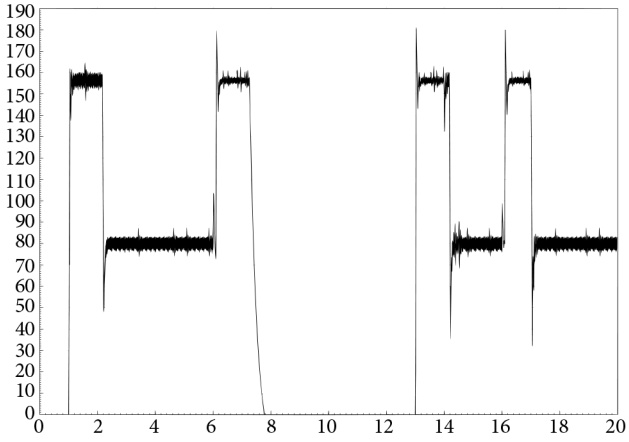


**Figure 10.** Output current in PROTEUS.

## 4. Implementation of inverter arc welding machine with the proposed converter

The circuit diagram of the developed 5 kW and 75 kHz single-phase soft-switched arc welding machine is shown in Figure 11. The circuit diagram mainly consists of the switching power supply (SMPS), DSP circuit, UC3879 circuit, auxiliary control circuit, and drive circuits. The nominal output current of the proposed welding machine is 160 A. The input voltage of the DC-DC converter is $V_d$ = 300 V, and operation frequency ($f_s$) is 75 kHz.

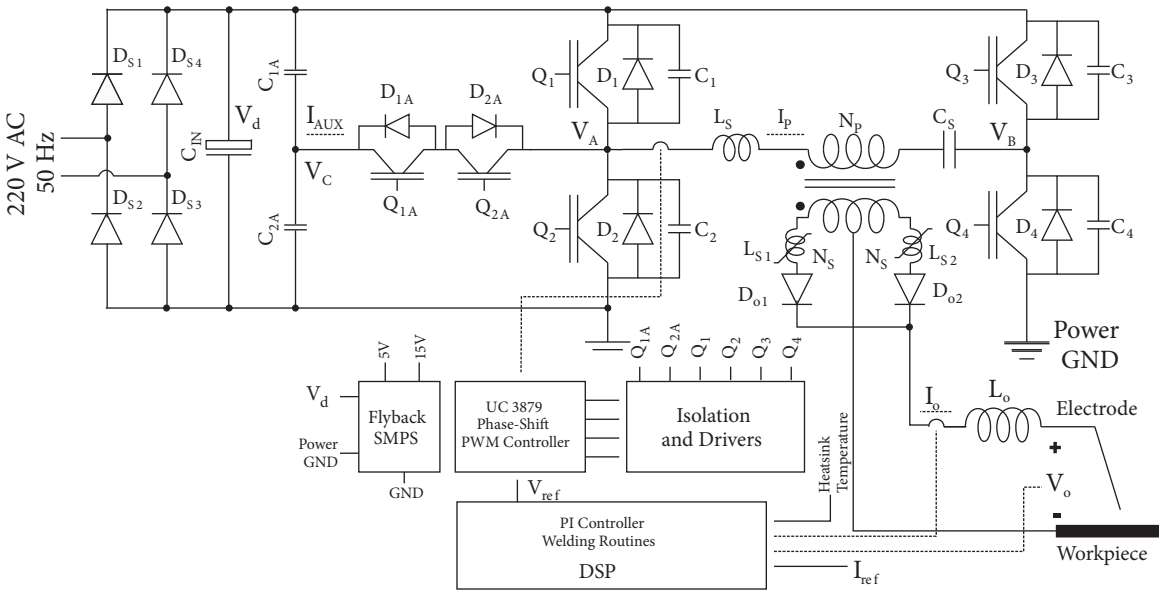


**Figure 11.** Experimental circuit scheme of the proposed arc welding machine.

In the simulation, the control of $V_{rec}$ voltage is realized with PWM output directly. In practice, in order to control the $V_{rec}$ voltage, the PWM output is converted to an analog value and then applied to UC3879 IC. Because DAC output is not available in DSP, the high-frequency PWM2 module of the DSP and the analog filter are used to obtain analog voltage representing $y$ output. The selected PWM frequency is 300 kHz. PWM output is filtered by the RC filter and converted to an analog value with a second-order low pass (LP) filter.

This analog output voltage ($V_{ref}$) is applied to UC3879 IC, and phase shift is adjusted by $V_{ref}$. UC3879 IC provides 0%–100% phase shift for a 1–4 V input voltage range.

The nominal values of the components used in the welding machine are listed in Table 1. The saturated inductances are connected in a series with the output diodes to prevent parasitic oscillations, which occur at the turn-off process of the output diodes. The voltage across the DC blocking capacitor $C_S$ is low because the capacitor value is high. Appropriate heat-sinks are used for power semiconductor devices, and the cooling is supported with a fan. Over-current, short-circuit, and temperature protection are implemented in the converter. Primary current is measured with a current transformer, and current information is given to the control IC for over-current protection. The current limit selected is 200 A.

**Table 1.** The nominal values of the components used in the welding machine.

| Item | Symbol | Value |
|---|---|---|
| Rectifier | $D_{S1}$–$D_{S4}$ | GBPC5008 |
| Input filter capacitor | $C_{IN}$ | 3 × 470 $\mu$F - 450 V |
| Main and auxiliary switches | $S_1$, $S_2$, $S_3$, $S_4$, $S_{1A}$ $S_{2A}$ | IXGH60N60C2D1 |
| Auxiliary circuit snubber capacitors | $C_{1A}$, $C_{2A}$ | 10 nF - 630 V |
| Lagging lag snubber capacitors | $C_1$, $C_2$ | 2.2 nF - 630 V |
| Leading lag snubber capacitors | $C_3$, $C_4$ | 10 nF - 630 V |
| Resonant inductor | $L_S$ | 5 $\mu$H |
| Transformer turns ratio | $N = N_P/N_S$ | 5:1 |
| Output diodes | $D_{o1}$, $D_{o2}$ | DSEI 2 × 121 |
| Output inductor | $L_o$ | 30 $\mu$H |
| Saturable inductor | $L_{S1}$, $L_{S2}$ | 10 $\mu$H |

The turn-off losses of the IGBT at a high current level are greatly reduced with the selection of the high-value capacitor. In the case of the high-value capacitor at no-load, switching devices can cause damage due to the discharge of the capacitors through the switches. The experimental tests realized for the turn-off process of the IGBT show that a parallel snubber capacitor value of around 20 nF minimizes turn-off losses of the selected IGBT. Selecting a high-value $L_S$ inductance maintains soft switching at low output currents. However, high-value inductance increases the reset time of the primary current; thus, the duty cycle losses increase and efficiency of the circuit decreases. In the application, $L_S$ and $C_S$ are high enough to avoid insufficient dead time.

The waveforms taken from the operating welding machine for different reference currents are shown in Figures 12–15. Welding current is kept constant by controlling the duty cycle. The regulation is provided against both arc voltage and DC bus voltage ripple.

Additional functions for initial and short-circuit cases are implemented with the welding algorithm. Output current and voltage are measured for the welding algorithm. The welding voltage ($V_o$) is the sum of arc voltage, the voltage on the wire resistance, and electrode resistance. The arc voltage is the largest component of the welding voltage.

In Figure 12, at the beginning of the welding process, the waveforms of $I_o$, $V_o$, and $V_d$ are given for $I_{ref}$ = 90 A. At no-load, $V_d$ is 300 V and the output voltage is 60 V, because duty is maximum. The welding process starts with the touch of the electrode to the piece. The welding current rises rapidly to the maximum value, and after the 2.5 ms hot-start duration it decreases to the reference value. Welding voltage decreases from 60 V to 20 V. If the welding process continues without a short circuit for a long time, a constant current flows through the electrode.

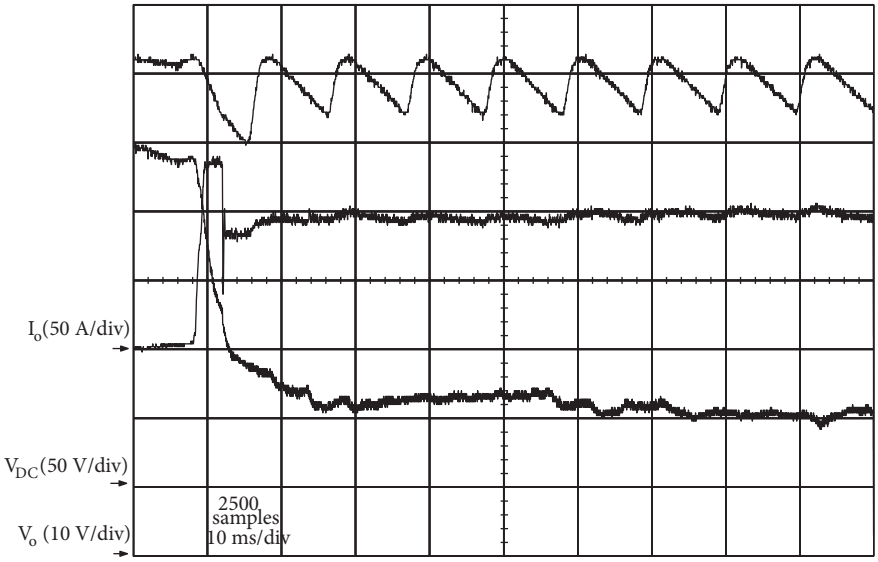


**Figure 12.** $I_o$, $V_o$, and $V_d$ waveforms for $I_{ref} = 90$ A.

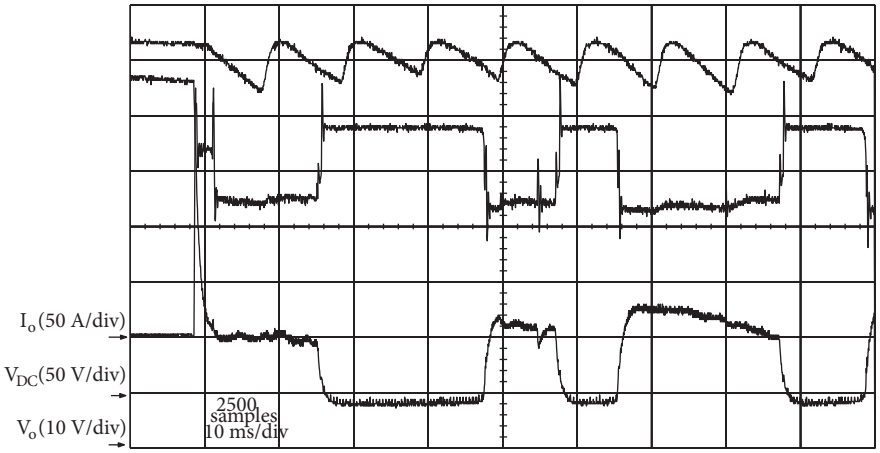


**Figure 13.** $I_o$, $V_o$, and $V_d$ waveforms for $I_{ref} = 125$ A.

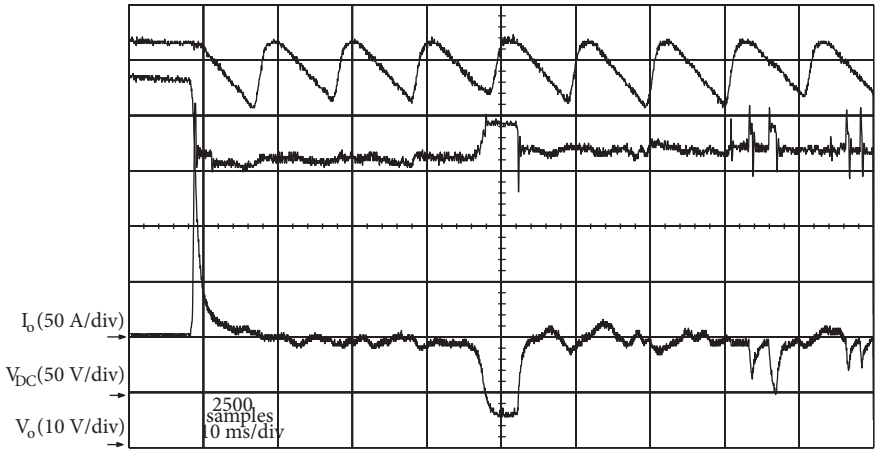


**Figure 14.** $I_o$, $V_o$, and $V_d$ waveforms for $I_{ref} = 160$ A.

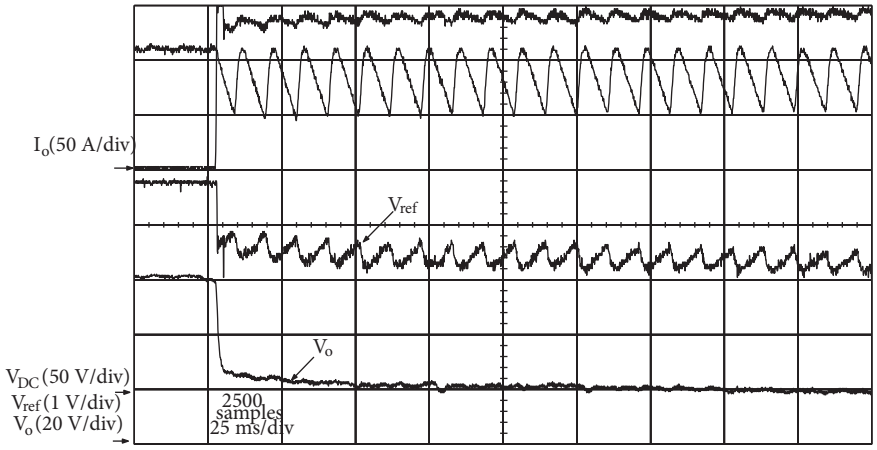


**Figure 15.** $I_o$, $V_o$, $V_d$, and $V_{ref}$ waveforms for $I_{ref}$ = 140 A.

Welding current regulation against the changes of the arc voltage and DC bus voltage is well provided. In Figure 13, $I_o$, $V_o$, and $V_d$ waveforms are shown for $I_{ref}$ = 125 A. From these waveforms it is seen that some short circuits occur due to the nature of arc welding. Short-circuit conditions are eliminated by making the current reference maximum. If the short-circuit duration is long, the current reference is reduced to zero, and the user can remove the electrode from the piece easily.

In Figure 14, $I_o$, $V_o$, and $V_d$ waveforms are shown for $I_{ref}$ = 160 A. The DC bus voltage ripple is 75 V, and the welding current tracks the reference current.

In Figure 15, waveforms of $I_o$, $V_o$, and $V_d$ are shown for $I_{ref}$ = 140 A. The welding current settles to the reference value. Welding voltage decreases from 60 V to 20 V, and it stays at about 20 V during the welding process. DC bus voltage ripple is 75 V. Control voltage ($V_{ref}$) is adjusted between 3.2 and 3.8 V, and welding current is kept constant.

Welding current ripple is due to fluctuations in DC bus voltage. This current ripple can be reduced by optimizing PI parameters. The current ripple is within normal ranges for arc welding. The current ripple is very high in conventional transformer welding machines and in most of the inverter welding machines. Various welding tests were successfully carried out with different electrode diameters and at different reference currents. The nominal current of welding machines is considered the continuous operating current of the machine. A welding machine shuts itself down due to overheating after operating for a certain period above the nominal current. When the internal temperature of the machine decreases to a normal level, the machine can be restarted. Temperature protection is mainly related to losses of the power semiconductor devices and high-frequency power transformer.

At nominal current the welding machine was operated for 60 min. After this test, the internal temperature was measured a thermal camera (FLIR i50), and some results are given in Figure 16.

The temperatures of some components are given in Table 2; the hottest component is the high-frequency power transformer.

The power diode temperature reaches very high values. The high temperature of the diode can be reduced by using a low conduction voltage drop diode or a larger heat-sink. The efficiency can be improved by reducing output rectifier losses.

The temperatures of the IGBT power switches are normal. Due to the operation principle of the converter, lagging leg switches are hotter than leading lag switches. In Figure 16 it is seen that the temperature of the resonance inductance is quite high. This is mainly due to copper losses, and this problem can be solved by using

larger diameters of wire. There is no important temperature increase for the output inductance and saturated inductances.


**Figure 16.** The thermal image of the welding machine after 60 min of nominal operation.

**Table 2.** Device temperature comparison after 60 min of nominal operation ($T_A$ = 30 °C).

| Device | Temperature (°C) |
|---|---|
| Input diodes | 130 |
| Power semiconductors | 76 |
| Transformer | 137 |
| Output inductance | 70 |
| Output diode | 100 |

The developed arc welding machine (DM) is compared with 2 commercial inverter welding machines (M1 and M2) at the same power level. The welding machine cannot be operated at its maximum current continuously. The duty of the welding machine is defined at different current levels in a 10-min period.

The continuous operating currents of M1, M2, and DM are 100 A, 130 A, and 140 A, respectively. For 60% duty ratio, M1, M2, and DM can supply 130 A, 160 A, and 160 A, respectively. The pulse frequency of the rectified output voltages of M1, M2, and DM are 40 kHz, 60 kHz, and 150 kHz, respectively.

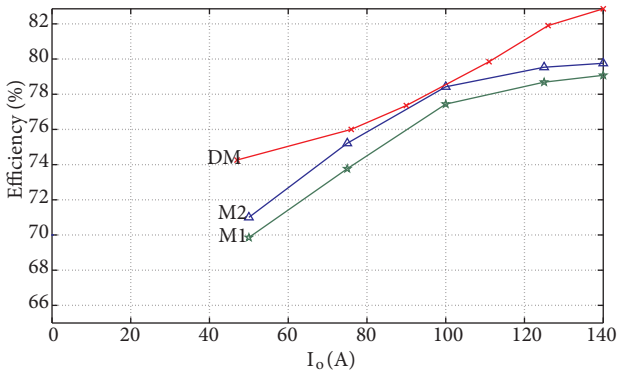


**Figure 17.** Efficiency comparison of the welding machines.

Efficiency curves of the arc welding machines are shown in Figure 17. The efficiency waveforms are obtained by measuring the input and output power of the welding machines. From Figure 17, it is seen that the developed welding machine has higher efficiency than the other machines. The efficiency of the developed welding machine is 83% at nominal output current.

## 5. Conclusions

In this study, a new single-phase inverter arc welding machine operating at 75 kHz switching frequency and 5 kW output power was presented. The power circuit was implemented with a high-frequency PSFB PWM converter. An electronic control card was designed, and the DSP software was developed for a welding machine. Some control functions such as PI current control, welding functions, fan control, relay control, and temperature control were implemented by using DSP software. By changing the duty cycle, the welding current was regulated against the changes in the arc voltage and DC bus voltage. Arc welding simulation was carried out with MATLAB and PROTEUS, and simulation results were confirmed with experimental results. The efficiency of the developed welding machine is 83% at nominal output current. This value is higher than those of the commercial welding machines it was compared with. Due to high-frequency operation and low loss, the developed welding machine has a low volume and high power density.

## References

[1] S. Buso, G. Spiazzi, F. Mela, S. Fasolo, "Design of an active load for electronic welding machines", Applied Power Electronics Conference and Exposition, pp. 1647–1653, 2009.

[2] C. Klumpner, M. Corbridge, "A two-stage power converter for welding applications with increased efficiency and reduced filtering", IEEE International Symposium on Industrial Electronics, pp. 251–256, 2008.

[3] J.A. Sabate, V. Vlatkovic, R.B. Ridley, F.C. Lee, B.H. Cho, "Design considerations for high-voltage high-power full-bridge zero voltage-switching PWM converter", IEEE-APEC, pp. 275–284, 1990.

[4] J.A. Sabate, V. Vlatkovic, R.B. Ridley, F.C. Lee, "High voltage, high-power, ZVS, full-bridge PWM converter employing an active snubber", IEEE-APEC, pp. 158–163, 1990.

[5] L.H. Mweene, C.A. Wright, M.F. Schlecht, "A 1 kW, 500 kHz front-end converter for a distributed power supply system", IEEE Transactions on Power Electronics, Vol. 6, pp. 398–407, 1991.

[6] R. Redl, N.O. Sokal, L. Balogh, "A novel soft-switching full-bridge DC/DC converter: analysis, design considerations, and experimental results at 1.5 kW, 100 kHz", IEEE Transactions on Power Electronics, Vol. 6, pp. 408–418, 1991.

[7] S. Hamada, M. Nakaoka, "Analysis and design of a saturable reactor assisted soft-switching full-bridge DC-DC converter", IEEE Transactions on Power Electronics, Vol. 9, pp. 309–317, 1994.

[8] J.G. Cho, "IGBT based zero voltage transition full bridge PWM converter for high power applications", IEE Proceedings - Electric Power Applications, Vol. 143, pp. 475–480, 1996.

[9] M. Nakaoka, S. Nagai, Y.J. Kim, Y. Ogino, Y. Murakami, "The state-of-the art phase-shifted ZVS-PWM series and parallel resonant DC-DC power converters using internal parasitic circuit components and new digital control", IEEE PESC, pp. 62–70, 1992.

[10] V. Vlatkovic, J.A. Sabate, R.B. Ridley, F.C. Lee, B.H. Cho, "Small-signal analysis of the phase-shifted PWM converter", IEEE Transactions on Power Electronics, Vol. 7, pp. 128–135, 1992.

[11] G. Hua, F.C. Lee, M.M. Jovanovic, "An improved full-bridge zero-voltage-switched PWM converter using a saturable inductor", IEEE Transactions on Power Electronics, Vol. 8, pp. 530–534, 1993.

[12] W. Tang, F.C. Lee, R.B. Ridley, "Small-signal modeling of average current-mode control", IEEE Transactions on Power Electronics, Vol. 8, pp. 112–119, 1993.

[13] J.G. Cho, J.A. Sabate, F.C. Lee, "Novel full bridge zero voltage-transition PWM DC/DC converter for high power applications", IEEE-APEC, pp. 143–149, 1994.

[14] R. Redl, L. Balogh, D.W. Edwards, "Optimum ZVS full-bridge DC/DC converter with PWM phase-shift control: analysis, design considerations, and experimentation", IEEE-APEC, pp. 159–165, 1994.

[15] I.D. Kin, E.C. Nho, G.H. Cho, "Novel constant frequency PWM DC/DC converter with zero voltage switching for both primary switches and secondary rectifying diodes", IEEE Transactions on Industrial Electronics, Vol. 39, pp. 444– 452, 1992.

[16] J.L.F. Vieira, G. Gabiatti, I. Barbi, "On the design and experimentation of a high performance 25 A, 48 V rectifier unit", IEEE-INTELEC, pp. 540–547, 1992.

[17] B.H. Kwon, J.H. Kim, G.Y. Jeong, "Full bridge soft switching PWM converter with saturable inductors at the secondary side", IEE Proceedings - Electric Power Applications, Vol. 146, pp. 117–122, 1999.

[18] R. Ayyanar, N. Mohan, "Novel soft-switching DC-DC converter with full ZVS-range and reduced filter requirement—part I : regulated-output applications", IEEE Transactions on Power Electronics, Vol. 16, pp. 184–192, 2001.

[19] X. Ruan, Y. Yan, "A novel zero-voltage and zero-current-switching PWM full-bridge converter using two diodes in series with the lagging leg", IEEE Transactions on Industrial Electronics, Vol. 48, pp. 777–785, 2001.

[20] S. Jeon, G.H. Cho, "A zero-voltage and zero-current switching full bridge DC-DC converter with transformer isolation", IEEE Transactions on Power Electronics, Vol. 16, pp. 573–580, 2001.

[21] C. Iannello, S. Luo, I. Batarseh, "Full bridge ZCS PWM converter for high-voltage high-power applications", IEEE Transactions on Aerospace and Electronic Systems, Vol. 38, pp. 515–526, 2002.

[22] E. Kim, Y. Kim, "A ZVZCS PWM FB DC/DC converter using a modified energy-recovery snubber", IEEE Transactions on Industrial Electronics, Vol. 49, pp. 1120–1127, 2002.

[23] G. Koo, G. Moon, M.Y. Youn, "New zero-voltage-switching phase-shift full-bridge converter with low conduction losses", IEEE Transactions on Industrial Electronics, Vol. 52, pp. 228–235, 2002.

[24] P.K. Jain, W. Kang, H. Soin, Y. Xi, "Analysis and design considerations of a load and line independent zero voltage switching full bridge DC/DC converter topology", IEEE Transactions on Power Electronics, Vol. 17, pp. 649–657, 2002.

[25] Y. Jang, M.M. Jovanovic, Y. Chang, "A new ZVS-PWM full-bridge converter", IEEE Transactions on Power Electronics, Vol. 18, pp. 1122–1129, 2003.

[26] J.M. Zhang, X.G. Xie, X.K. Wu, Z. Qian, "Comparison study of phase-shifted full bridge ZVS converters", IEEE-PESC, pp. 533–539, 2004.

[27] S. Moisseev, K. Soshin, S. Sato, L. Gamage, M. Nakaoka, "Novel soft-commutation DC-DC power converter with high-frequency transformer secondary side phase-shifted PWM active rectifier", IEE Proceedings - Electric Power Applications, Vol. 151, pp. 260–267, 2004.

[28] Y. Jang, M.M. Jovanovic, "A new family of full-bridge ZVS converters", IEEE Transactions on Power Electronics, Vol. 19, pp. 701–708, 2004.

[29] S. Sato, S. Moisseev, M. Nakaoka, "Reversed-output current-assisted ZVS phase-shift PWM DC-DC power converter using synchronous rectifier", IEE Proceedings - Electric Power Applications, Vol. 152, pp. 423–428, 2005.

[30] A.F. Bakan, İ. Aksoy, N. Altıntaş, H. Bodur, "Comparison of the full bridge PSPWM DC-DC converters", Proceedings of ETAI Conference, 2009.

[31] A.F. Bakan, İ. Aksoy, N. Altıntaş, H. Bodur, "Tam köprü PSPWM DC-DC dönüştürücülerin karşılaştırılması", International Conference on Electrical and Electronics Engineering, 2008 (in Turkish).

[32] A.F. Bakan, "A new PSPWM converter for high performance welding machines", International Universities Power Engineering Conference, pp. 1–5, 2009.

[33] A.F. Bakan, İ. Aksoy, N. Altıntaş, H. Bodur, "An experimental investigation of switching losses of the IGBT in PSPWM DC-DC converters depending on the parallel snubber capacitor", Proceedings of ETAI Conference, 2009.

[34] A.F. Bakan, H. Bodur, İ. Aksoy, N. Altıntaş, "IGBT tabanlı tam köprü PSPWM DC-DC dönüştürücüde bastırma kondansatörlerinin belirlenmesi", International Conference on Electrical and Electronics Engineering, 2008 (in Turkish).

[35] A.F. Bakan, "A new LVI assisted PSPWM DC-DC converter", International Conference on Electrical and Electronics Engineering, pp. I-230–I-233, 2009.

[36] A.F. Bakan, H. İşbilir, İ. Aksoy, N. Altıntaş, H. Bodur, "Drive transformer design for phase shifted PWM DC-DC converters", Proceedings of ETAI Conference, 2009.

[37] C.B. Yuan, L.Y. Shin, "Switching control technique of phase-shift-controlled full-bridge converter to improve efficiency under light-load and standby conditions without additional auxiliary components", IEEE Transactions on Power Electronics, Vol. 25, pp. 1001–1012, 2010.

[38] Z. Xin, H.S. Chung, R. Xinbo, A. Ioinovici, "A ZCS full-bridge converter without voltage overstress on the switches", IEEE Transactions on Power Electronics, Vol. 25, pp. 686–698, 2010.

[39] J.M. Wang, S.T. Wu, S.C. Yen, H.J. Chiu, "A simple inverter for arc-welding machines with current doubler rectifier", IEEE Transactions on Industrial Electronics, Vol. 58, pp. 5278–5281, 2011.

[40] K. Lo, C. Lin, T. Hsieh, Y. Lin, "Phase-shifted full-bridge series-resonant DC-DC converters for wide load variations", IEEE Transactions on Industrial Electronics, Vol. 58, pp. 2572–2575, 2011.

[41] N. Blasco, A. Martinez, F.J. Cebolla, J.E. Vicuna, I. Lacamara, J.A. Oliva, "Evaluation of power converters for MMA arc welding", IEEE International Symposium on Industrial Electronics, pp. 365–370, 2007.

[42] A.F. Bakan, N. Altıntaş, İ. Aksoy, "An improved PSFB PWM DC-DC converter for high-power and frequency applications", IEEE Transactions on Power Electronics, Vol. 28, pp. 64–74, 2013.